International Journal of Applied Earth Observation and Geoinformation 141 (2025) 104670

Contents lists available at ScienceDirect

International Journal of Applied Earth Observation and Geoinformation

journal homepage: www.elsevier.com/locate/jag

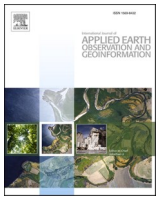

A cloud-based framework for the quantification of the spatially-explicit uncertainty of remotely sensed benthic habitats☆

Spyridon Christofilakos [a,*], Alina Blume [a,c], Avi Putri Pertiwi [a], Chengfa Benjamin Lee [a], Dimosthenis Traganos [b], Peter Reinartz [d]

[a] German Aerospace Center (DLR), Earth Observation Center (EOC), Remote Sensing Technology Institute (IMF), Imaging Spectroscopy Department, Germany
[b] German Aerospace Center (DLR), Earth Observation Center (EOC), Remote Sensing Technology Institute (IMF), Department of Photogrammetry and Image Analysis, Rutherfordstraße 2, 12489 Berlin, Germany
[c] European Space Agency (ESA), ESA-ESRIN, Largo Galileo Galilei 1, 00044 Frascati, Italy
[d] German Aerospace Center (DLR), Earth Observation Center (EOC), Remote Sensing Technology Institute (IMF), 82234 Weßling, Germany

ARTICLE INFO

Keywords:
Seagrass
Random forest
Cloud-computing
Thematic mapping
Model retraining

ABSTRACT

The significant advances of cloud-based remote sensing frameworks have allowed researchers to develop large-scale analytics for better understanding, monitoring of, and decision-making around sensitive and valuable coastal ecosystems like seagrass meadows. However, an information gap related with the spatially-explicit accuracy of Machine Learning (ML) products has been identified. The goal of this study is to estimate the per pixel uncertainty of a Random Forest classification of four benthic habitats and exploit it to retrain the model through training data selection by bootstrapping and producing an ensemble model. The calculation of the spatially-explicit uncertainty is based on the Shannon Entropy equation and the probability values of a successful prediction according to the ML model. The remote sensing data for this study are sourced from the European Union Copernicus Sentinel-2 twin satellite system and Planet's cubesat satellite constellation respectively, and have been processed and analyzed through the Google Earth Engine cloud-based platform. The national extent of The Bahamas and the regional extent of the Wakatobi archipelago in Indonesia comprise our study sites. Our results indicate the potential of the presented uncertainty workflow for optimizing the classification and the usefulness of the produced uncertainty map to aid policy-makers through our provided spatially-explicit accuracy metrics. More precisely in the case of the Bahamas, the percentile differences for seagrass user and producer accuracies are improved in the ranges of 1.16–4.77 % and 4.36–8.54 %, respectively, in comparison with a standard supervised classification. In conclusion, spatially-explicit uncertainty information can and should be used as unique and vital geospatial information suitable for ML classification optimization and as a tool for better decision-making and field expedition planning, and understanding of benthic ecosystems.

1. Introduction

As seagrass meadows are declining globally, new and robust techniques need to be developed for large scale mapping and monitoring, in order to aid policy makers to sustain these millennial ocean ecosystem service providers (Papenbrock and Teichberg, 2023; Litsi-Mizan et al., 2023; Orth and Heck, 2023). Seagrass contributes to the reduction of coastline erosion by absorbing kinetic wave energy (Infantes et al., 2022; Paul, 2018; Potouroglou et al., 2017). In addition, seagrass maintains biodiversity by providing shelter and nursery grounds to intertidal and subtidal coastal life, and, most importantly, contributing to blue carbon sequestration (Unsworth et al., 2019; Duffy, 2006; Duarte, 2002). It removes carbon from the atmosphere and water column, and deposits it in its deep root system and the surrounding soil (Lavery et al., 2013; Duarte et al., 2005). For these reasons, the mapping of seagrass habitats is behoved due to its support of the Sustainable Development Goals (SDGs) for the coastal environment and the need for solid and transparent Nationally Determined Contributions (NDCs) for mitigating climate change (United Nations, 2015). Earth Observation (EO) contributions constitute one of the main ways to achieve this

☆ This article is part of a special issue entitled: 'Spatially Explicit ML&AI' published in International Journal of Applied Earth Observation and Geoinformation.

* Corresponding author.
E-mail address: spyridon.christofilakos@dlr.de (S. Christofilakos).

https://doi.org/10.1016/j.jag.2025.104670
Received 27 October 2023; Received in revised form 11 March 2025; Accepted 9 June 2025
Available online 13 June 2025

objective. Compared to field studies, EO features much greater temporal and spatial scalability, and can monitor seagrass meadows across multi-decadal time scales, and in vast and remote regions, all over the globe.

A plethora of scientific studies showcases the use of EO data for mapping and monitoring seagrass meadows (Hossain and Hashim, 2019; Poursanidis et al., 2018). In the last decade, seagrass mapping has been on the rise in coastal remote sensing studies globally. From mapping seagrass meadows with Sentinel-2 data in the Baltic Sea (Kuhwald et al., 2022) and the Bahamian archipelago (Blume et al.,2023), to mapping the whole seagrass extent of East Africa (Traganos et al., 2022b) and the Mediterranean Sea (Traganos et al., 2022a), and even detecting seagrass patches up to the depth of 32.2 m (Poursanidis et al., 2019). Li et al. (2021) and Traganos et al. (2018) highlight the importance and robustness of cloud-based platforms such as Google Earth Engine (GEE) for such tasks and how it aided the mapping of coastal China, and the Aegean and Ionian seas of Greece (Li et al., 2022; Traganos et al., 2018). Likewise, the Allen Coral Atlas (ACA) has provided scalable global benthic and geomorphic maps for the tropics with PlanetScope data and proves the value of GEE for projects utilizing big data (Lyons et al., 2022).

Regarding the accuracy of EO products to date, there is an undeniably continuous progress on the side of pre-processing of big data (enormous size of data due to time series analysis, creation of multi-temporal composites for national and continental study areas, etc.), and the cutting-edge Machine Learning (ML) and Deep Learning (DL) procedures, resulting in considerably high accuracies. For example, the overall accuracies of the Mediterranean and Bahamian seagrass maps are 72 % and ~76 %, respectively (Blume et al., 2022; Traganos et al., 2022). In a study in coastal locations in Florida, Convolutional Neural Network (CNNs) were able to achieve accuracies in the range of 93 % to 99 %, depending on the number of training patches, due to their intensive self-training properties and the use of very high spatial resolution 1-m WorldView-2 datasets (Perez et al., 2020). In general, scientists, researchers and policy-makers are experimenting with a number of different remote sensing sensors like Landsat-8, Sentinel-2, and Planet datasets, among others, and in some cases even Unmanned Aerial Vehicles (UAVs), to achieve an accurate mapping of seagrass extent (Lee et al., 2023; Doukari and Topouzelis, 2022; Topouzelis et al., 2018; Kovacs et al., 2018). However, there is an information gap in the spatially-explicit level of these vanguard approaches as there is a limitation on the assessment of large-scale application (Velegrakis et al., 2024) due to the need of spatially-bounded ground-truth data (Sayer et al., 2020; Tran et al., 2023). This gap is related to the quantifiable per pixel uncertainty of the machine learning products. This per pixel information can potentially aid policy makers with critical decision-making insights and in addition, in the context of computer science, can optimize the accuracies of machine and deep learning products.

Within this context, Poursanidis et al. (2018) estimated the per pixel uncertainty based on Shannon's Entropy (Shannon, 1948) while mapping seagrass meadows in three coastal areas in Greece by using the downscaled coastal aerosol band of Sentinel-2. By following a Bayesian perspective, quantified the predictive uncertainty with ensembles of CNNs for their global canopy height estimation with National Aeronautics and Space Administration's (NASA) GEDI system (Lang et al., 2022). In the same direction, Guerrero-Font et al. (2021) proposed a method to map uncertainty linked with spatial distribution of seagrass with Gaussian Processes and data gathered by an autonomous vehicle. Despite these efforts, a proper tool to aid policy making and field measurements, and Artificial Intelligence (AI) optimization based on the spatially-explicit uncertainty information of machine learning products has not been developed yet.

The aim of this study is to develop a cloud-based semi-automated workflow for the estimation of the spatially-explicit uncertainty of ML classification procedures targeting coastal ecosystems. Spatially-explicit uncertainty refers to the quantification of uncertainty that varies across locations within a study area, enabling a detailed, pixel-based assessment of the classification model's confidence in each prediction. The motivation for this study is to establish a practical quality indicator of high-confidence seagrass classifications, which in turn can optimize the whole procedure by filtering training data based on their entropy levels that results in the reduction of the introduced noise in the model.

2. Methodology

2.1. Study sites

This scientific paper investigates the implementation of spatially-explicit uncertainty in a coastal remote sensing study conducted across two distinct study sites and geographical scales: the national extent of The Bahamas and the regional extent of the Wakatobi archipelago in Indonesia. A number of studies in both coastal systems and geographical scales argue the importance of protecting them due to their high biodiversity and blue carbon storage potential (ECLAC and CDCC, 2020, Alongi et al., 2016) These sites unfortunately face various challenges such as coastal ecosystem degradation, shoreline erosion, and pollution (Ferrol-Schulte et al., 2015; Edinger et al., 1998). Their tropical location is also a challenge for remote sensing scientists due to yearlong persistent cloud cover and limited field measurements. Therefore, these areas were chosen to assess the potential of the presented workflow via a data driven approach without intensive pre-processing parameterization. By incorporating uncertainty analysis into the classification of these sites, a more comprehensive understanding of the collected data and their inherent uncertainties and limitations can be achieved.

The coastal region of The Bahamas exhibits dynamic oceanic processes influenced by several factors, including ocean currents, tides, and wave patterns (Slattery and Lesser, 2019). As Slattery and Lesser (2019) described, the warm waters of the Gulf Stream interact with the complex bathymetry and coastline of The Bahamas, resulting in complex flow patterns that impact the distribution and transport of nutrients, sediments, and coastal organisms. These driving ocean dynamics contribute to the rich biodiversity and productivity of coastal ecosystems making Bahamian seagrasses one of the biggest ecosystems in size, in continuous meadows terms, globally (Blume et al., 2023; Gallagher et al., 2022). In addition, the three regional seagrass species are *Thalassia testudinum, Syringodium filiforme, Halodule wrightii* (Blume et al., 2023).

Concerning the islands of Wakatobi, Indonesia, there is a complex interplay of oceanic processes influenced by factors like seasonal monsoons, currents, and bathymetry (Sprintall et al., 2014). The region experiences strong tidal regimes and the influence of the Indonesian Throughflow ocean current, which contributes to significant variations in water temperature, nutrient distribution, and sediment transport (Taufiqurrahman et al., 2020; Ayers et al., 2014). In turn, the Wakatobi archipelago features diverse coastal ecosystems of—vibrant coral reefs, seagrass beds, and mangrove forests. Concerning seagrasses, there are 12 species in total in Indonesia, with *Thalassia hemprichii* and *Enhalus acoroides* being the most abundant ones (Unsworth et al., 2010). Moreover, these meadows provide shelter and feeding grounds to 188 fish species. Similar to The Bahamas, Indonesia processes a crucial part of the world's blue carbon stocks and sequestration rates as its seagrasses and mangroves hold roughly 17 % of the world's blue carbon reservoir (Alongi et al., 2016).

2.2. Satellite and reference data

The adjustability of the workflow in satellite data input is assessed by processing two individual satellite data sets to produce the coastal habitat classification and uncertainty maps.

The first satellite sensor is the European Space Agency's twin-satellite mission Copernicus Sentinel-2 (S2), a well-known instrument for its performance in coastal remote sensing studies, despite its terrestrial based radiometric correction (Pahlevan et al., 2021; Louis

et al., 2019; Doxani et al., 2018; Gascon et al., 2017). In the case of The Bahamas, S2′s first four bands of Blume et al. (2023)'s image composite were used to run an Object-based image analysis (OBIA). The OBIA product is an image with 5-pixel sized objects whose values are the mean, median and standard deviation of the included pixels of the bands are shown in Table 1. The advantage of using OBIA over pixel-based classification lies in capability to handle the complex nature of benthic habitats, yielding accurate and reliable results (Hartoni et al., 2021; Panjaitan and Hamidah, 2023) as it goes beyond pixel-level analysis by considering the spatial relationships and interactions between neighbouring pixels (Blaschke et al., 2014).

The second satellite source that supports classification efforts in Wakatobi is Planet's cube satellite constellation (Planet Labs PBC, 2018) also known for their coastal remote sensing application (Lee et al., 2023; Zhang et al., 2023; Wicaksono and Lazuardi, 2018). Under an agreement with Norway's International Climate and Forests Initiative (NICFI), Planet Labs provide free access through GEE to high resolution and analysis-ready, biannual mosaics in the Tropics.[1] As with S2 data, the Planet NICFI data were processed to produce the Depth InVariant Index (DIV), hue and value bands and another OBIA composite. In the case of Wakatobi, like in similar studies that we worked on (Lee et al., 2022; Pertiwi et al., 2021), the land mask incorporates the Otsu algorithm to distinguish land from water based on values of the Modified Normalized Difference Water index (MNDWI) (Donchyts et al., 2016). Otsu's method automatically determines the optimal threshold values by identifying those that minimize the intra-class variance within image histogram (Otsu, 1979).

The reference data of this study consistof two point collections that differ for each study site. The first collection is the training data which train the classifier to map four benthic habitats: seagrass, sand, corals, and rock. The second collection is the validation data, which evaluate the accuracy of the classification model. The training data for both study sites were sampled from the ACA[2] data product. For The Bahamas, the validation data were based on multiple data sources leveraging field data acquisitions with remotely sensed covariates, aggregated throughout the entire Bahamas (Roelfsema et al., 2021). In contrast, for Wakatobi, the validation dataset was sourced from the ACA data product due to the absence of a reliable and publicly available dataset. As both the training and validation datasets originate from the same source, some degree of model overestimation is expected. The Tables 1 and 2 provide the characteristics of the created features and satellite data used for the classification respectively.

2.3. Workflow in brief

The workflow of this study is divided into three stages and is conducted entirely within GEE due to its scalability and computing power,

Table 1
Created features for the classification.

Bands	Physical Properties
B1(resampled to 10 m), B2, B3, B4	Spectral Reflectance on the wavelengths B1: (442.3–443.9 nm), B2: (492.1–496.6 nm), B3: (559–560 nm), B4: (664.5–665 nm)[a]
DIV	Depth Invariant Index (Lyzenga,1981)
Hue, Value	Hue: Color, Value: Refers to the brightness of color (Lee et al., 2022)

[a] https://sentinel.esa.int/web/sentinel/user-guides/sentinel-2-msi/resolutions/spectral.

[1] https://www.planet.com/nicfi/?gad=1&gclid=CjwKCAjwhdWkBhBZEiwA1ibLmGN92mBe4-2VRs8fv6Kzza2jlBeElt1WRuKfzVAVZT6027P2G8iG3hoCGnMQAvD_BwE&restored=1687525741028.

[2] https://allencoralatlas.org/.

Table 2
Satellite data for the classification.

	Spatial resolution (m)	Time resolution (days)	# of Satellite images	Length of time-series
Sentinel-2	10	5	18,881 images	4 years (2017–2021)
Planet NICFI	5	1	10 biannual and 4 monthly composites[a]	5 (2015–2020)

[a] Mid-year of 2020 Planet starts to provide monthly composites.

which allows the user to process vast amount of remote sensing data quickly and efficiently. Notably, by the end of stage two, the total file size of the byproducts reaches approximately 192.74 GB. The first stage pre-processes the reference data and separates them to training (90 %) and validation (10 %) data as six and one subsets respectively. Then, the training subsets are bootstrapped six times and initiate the second stage which optimizes the classification outcome in a data driven way based on the spatially-explicit uncertainty values of the individual classifications and their training data. The use of multiple data subsets aims to establish a structured retraining framework with balanced training data for each class and to explore the approach's limitations. Preliminary, unpublished experiments indicate that a single retraining consistently yields improved results by reducing data-induced noise. The second stage is the retraining stage. Last, in the third stage, a single ensemble model is created based on the mode value of the bootstrap loop products.

2.4. Spatially-explicit uncertainty

In this study, uncertainty was treated under a Bayesian perspective. Therefore, its estimation depends on the prior knowledge of the probabilities of success for each possible classification outcome, a process known as soft classification. These probabilities are accessible via GEE, allowing the classifier to provide the probability of each class instead of the typical discrete distribution used in hard classification. Thus, the per-Pixel Uncertainty (PUNC) is estimated based on the alteration of the Shannon's Entropy Equation:

$$H(X) = -\sum_{i=1}^{n} p(x_i) log_2 p(x_i)$$

where: $H(X)$ = Pixel UNCertainty (PUNC)
$p(x_i)$ = Probability of Classification Success per Pixel,
x_i= Classification Value per Pixel.
$_i$=Classification Class: {[1,4]}.

The range of values for $H(X)$ depends on the number of classes for which, in this case, the maximum H(X) value is two. Based on that, by dividing the value of $H(X)$ by two, the range of values is rearranged to [0,1].

2.5. Retraining stage

The retraining stage consists of six loops in agreement with the size of the subsets.

The workflow is divided into three stages (Fig. 1). The first step of the second stage, from now on referred to as "initial classification", takes place in the first loop where a classification takes place with one out of the six subsets with the usage of Random Forest classifier (Pal, 2005; Breiman, 2001). Given that the primary goal of this paper is to establish PUNC information as a pixel-scale performance metric for high-confidence classifications in coastal zones and subsequently utilize it to optimize classification outcomes, we did not prioritize tuning the classifier's parameters. Consequently, the classification model remains as simple as possible by experimenting with 15 and 50 trees. Then, PUNC values are estimated as described in the previous paragraph. The

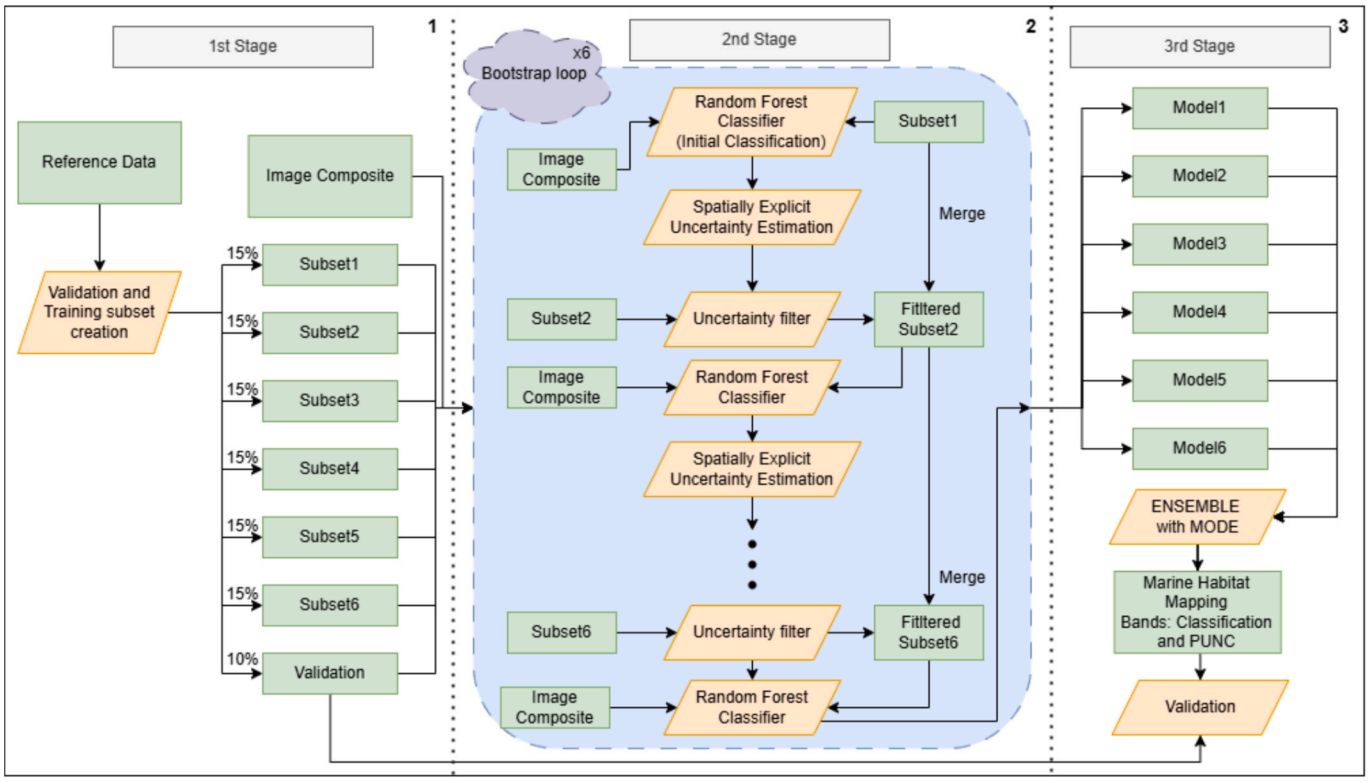

Fig. 1. Schematic workflow of developed uncertainty and re-trained framework.

second step contains an uncertainty filter that is applied to all remaining subsets and retains training data with uncertainty values less than 0.25, 0.75, 0.90 and bigger than 0.75. The reason for these four uncertainty thresholds investigates three hypotheses: a) to what extent certain training data with PUNC value less than 0.25 strengthens the model; b) minimizes the introduction of noise to the model by allowing retraining with training data with PUNC values less than 0.75 and 0.90; and c) if retrained training data with uncertainty higher than 0.75 aids the classifier to distinguish similar spectral signatures (e.g. coral – seagrass, optical deep sand – seagrass, rock – coral, etc.).

With the filtered data in place, the second step concludes with six classifications, each using unbalanced, individual training data. The training datasets for the six classifications are created by combining the subset used in the initial classification with a different filtered subset. The third and last step concludes with six models. These models are the products of a sequential retraining and reclassification with the only difference among them being the initial and unfiltered training subset.

2.6. Alternative retraining

Under the context of exploring new ways to use PUNC for optimizing the classifier, larger initial subsets and alternative uncertainty thresholds were applied. Larger initial subsets mean the merging of two subsets during the initial classification, leaving to perform four retrainings compared with the five from section 2.5. Additionally, we replace the uncertainty thresholds with five alternative values (>0.5, <0.5, >0.75, <0.75, <0.9). The term alternative stands for the changes of i) the uncertainty thresholds between the retrainings (Supplementary Material) and ii) the training subsets among the retraining phase. The latter is displayed in the following table (Table 3).

As explained earlier, this paper does not prioritize tuning classifier's parameters; therefore, classifications employing 50 Random Forest trees are not examined in the context of alternative retraining due to memory and time constraints.

Table 3
The alternative subsets and how their order of application during the retraining phase.

subsets for initial classification	subset for1st retraining	subset for2nd retraining	subset for 3rd retraining	subset for4th retraining
1 & 2	3	4	5	6
3 & 4	5	6	1	2
5 & 6	3	4	1	2
1 & 6	3	4	5	2
2 & 5	3	4	1	2

2.7. Ensemble models: The mode, the models, and the uncertainty

At the end of the retraining, the size of the produced models from the Retraining Stage and Alternative Retraining are six and five models, respectively. These models compile the dataset on which the most frequent value is chosen as the final classification value. Meanwhile, the PUNC value of the ensemble classifier is the average PUNC value of the models. According to literature, the mean value of PUNC serves as the epistemic uncertainty while its variance as the aleatoric uncertainty (Lang et al., 2022).

2.8. Accuracy assessment

The validation of the products is based on well-established metrics in remote sensing studies: overall accuracy, F1 score, user's and producer's accuracy. Then, accuracy scores of the ensemble models are compared with the scores of an independent classification trained with the entire training dataset (Tables 7 & 8).User's and producer's accuracies provide the commission and omission errors, respectively. Both the commission and omission errors show the misclassified validation data points. The commission errors can be used as an indicator of overestimated datasets over a class, whereas omission errors can be used as an indicator of

underestimated datasets.

3. Results

3.1. Bahamas results

The overall accuracy of the classification with all training dataset points ('All data' column in Tables 4 & 5) is 59.8 % with the parameter of trees for the Random Forest set as 15, and 61.2 % when the trees parameter is 50 (Table 4). A slightly better accuracy (60.3 %) is achieved only when the trees parameter is 15 and an uncertainty threshold less than 0.90 during the filtering of the training subsets in each loop is used. As for models retrained with certain data uncertainty thresholds less than 0.75 and 0.25, the overall accuracies are not improved.

3.2. Wakatobi results

In the case of classifications in Wakatobi (Table 5), however, retraining the models with medium to high uncertainty training points leads to a reduction of the overall accuracy of the classification with the whole dataset in a range of values: 0.014–0.04 %. Similar to the classifications in The Bahamas, the worst result of the Wakatobi classifications arises from the retraining based on training data with low PUNC. In this case, the classifier uses 15 trees. Nevertheless, for Wakatobi, the accuracy results should not be considered due to the overestimation arising from the use of the same source for both training and validation data. The accuracy results are presented to assess how the proposed method optimizes the model and it applicability to PLANET data.

3.3. Alternative retraining

3.3.1. Bahamas

Among the 125 produced models, the 64.8 % (81 models) achieves higher overall accuracy compared to the 59.83 % of the 'All Data' classification, which was obtained using the whole training dataset and 15 number of trees for RF. Of these 81 models, the 23.5 % had their first retraining done with PUNC <0.9, the 39.5 % with PUNC <0.75 or PUNC > 0.75, and the remaining 37 % with PUNC <0.5 or PUNC >0.5. Additionally, the mean overall accuracy of the 125 produced models is 60.25 %, exceeding the 'All Data' classification by 0.414 (Table 6).

According to our findings, the presented uncertainty workflow is able to slightly boost user's and procurer's accuracy values of seagrass and coral classes significantly (Table 7), despite the minor improvement of 1.67 % in the overall accuracy. A table with the exact accuracies and the mean PUNC per class is available at the Supplementary Materials. From the data in Table 7, it can be seen that the coral class is the one with the most positive impact as its user's accuracy achieves a percentile difference in the range of 11.79 % and 13.84 %. Additionally, a comparison of the confusion matrices for the 'All Data' classification and the Best Ensemble Model (available in Supplementary Material) reveals a 4 % decrease in seagrass validation points misclassified as coral. Interestingly, the average PUNC for all classes increases following the application the presented method, with Sand class showing the largest percentile difference and the coral class the smallest (see Fig. 2).

Table 4
Results of the classification given a constant uncertainty threshold. All data stands for a classification with the whole training set.

Number of trees	Uncertainty threshold for subset filtering				
	<0.25	<0.75	>0.75	<0.90	All data
15 trees	59.5 %	57.4 %	59.4 %	60.3 %	59.8 %
50 trees	57.1 %	57.8 %	59.8 %	59.4 %	61.2 %

Table 5
Results of the classification in Wakatobi given a constant uncertainty threshold. All data stands for a classification with the whole training set.

Number of trees	Uncertainty threshold for subset filtering				
	<0.25	<0.75	>0.75	<0.90	All data
15 trees	98.2 %	98.9 %	99.2 %	99.2 %	99.5 %
50 trees	98.7 %	98.5 %	99.2 %	99.3 %	99.2 %

Table 6
The best three models of the alternative retraining in The Bahamas and their respective uncertainty thresholds during each retraining. Main criteria for the selection are the Overall Accuracy and User's Accuracy of the seagrass class.

Alternative Retraining best models (2)	Overall Accuracy [%]	Uncertainty threshold for the 1st retraining	Uncertainty threshold for the 2nd and 3rd retraining	Uncertainty threshold for the 4th retraining
1.	61.5	< 0.75	> 0.75	> 0.50
2.	61.25	< 0.50	< 0.50	> 0.75
3.	61.33	< 0.75	< 0.75	> 0.75

3.3.2. Wakatobi

In the case of the Wakatobi classifications (Fig. 3), the alternative retraining is not capable of providing better results. In the following table, a minor improvement of user's accuracy in the class of coral is observed which leads to a reduction of the producer's accuracy when user's accuracy peaks.

However, these results cannot be taken in consideration in context of classification due to the same data pool of training and validation data, which leads to inflated accuracy.

4. Discussion

4.1. Uncertainty information and its value for EO

The main aims of this study are to produce a spatially-explicit uncertainty map and investigate its usage for optimization of GEE-based ML classifications. To our best knowledge, this is the first study to present a scalable approach for spatially-explicit estimation and mapping of uncertainty for coastal habitats in regional and national scale. The results indicate the efficacy of the presented approach due to its adjustability to two different satellite sensors and geographical scales. Even though the accuracy of the ensemble model in the classification in The Bahamas is not significantly better than the accuracy of the 'All data' classification, the producer's and user's accuracies of the classes with the most ecological interest, namely seagrass and coral are slightly and significantly higher, respectively. In conjunction with the presented retraining and alternative retraining approaches and based on the produced uncertainty map, our findings support the value of a spatially-explicit uncertainty map. Thus, a new pathway for future studies on ML optimization, decision making based on uncertainty knowledge and even environmental impact assessment, shall be made available. The produced geospatial information of uncertainty is in position to highlight regions where the classification model is less certain as in other regions due to similar spectral signatures of the classes and/or signatures which are not represented enough in the training dataset. Researchers will be able to better optimize their field data sampling by providing recommendations to increase the sampling in these uncertain areas and/or reducing the data points located in the certain areas depending on the case study. These insights shall be able to advise researchers to re-design their future in-situ expeditions accordingly. Under the current perspective of policy makers, the PUNC value may help to set the boundaries of protected areas with more certainty than standard remote-sensing classification methods.

Table 7
Accuracy Metrics for comparison based on the percentile difference between the best three ensemble models of the alternative retraining in The Bahamas and a standard classification using all the data from training data.

Percentile Difference (%)	Best Ensemble Model	Second Best Ensemble Model	Third Best Ensemble Model
Overall Accuracy	2.75	2.34	2.48
F1	2.61	2.33	2.75
Average PUNC Seagrass	2.15	3.63	1.14
User's Accuracy Seagrass	1.16	4.77	1.71
Producer's Accuracy Seagrass	6.77	8.54	4.36
Average PUNC Sand	6.75	5.20	5.38
User's Accuracy Sand	-0.39	-0.40	0.80
Producer's Accuracy Sand	0.42	0.00	-0.42
Average PUNC Coral	0.21	1.60	0.50
User's Accuracy Coral	13.84	11.79	12.95
Producer's Accuracy Coral	7.41	5.35	13.33
Average PUNC Rock	4.49	4.25	3.60
User's Accuracy Rock	0.66	-2.01	0.72
Producer's Accuracy Rock	0.43	-0.87	-0.44

Table 8
Accuracy Metrics for comparison between the best two ensemble models of the alternative retraining in Wakatobi and a standard classification using all the data from training data.

Classification model	Overall Accuracy [%]	User's accuracy (seagrass) [%]	Producer's accuracy (seagrass) [%]	User's accuracy (coral) [%]	Producer's accuracy (coral) [%]
Best Ensemble model	99.5	1	1	1	98.2
Second Best Ensemble model	99.5	1	1	98.2	1
Classification with All Data	99.5	1	1	98.1	1

4.2. Uncertainty of classification and its perception

The main goal of PUNC estimation is to support policy-making decisions and utilize it for model optimization, which we have showcased through our results. Unfortunately, slightly better produced accuracies based on the alternative retraining classifications were achieved only in our classification in The Bahamas but not in Wakatobi. However, all results indicate the potential of the presented approach for serving as a loss function for training data selection and providing spatial information on the accuracy of a classification for optimal decision making on thresholding and monitoring marine protected areas. This 'best data' selection insight would not be possible without the estimation of the spatially-explicit uncertainty information as it provides a behind-the-curtains relationship between the ground truth data location and the spectral signature of the corresponding pixel with the predicted class. This relationship suggests how noisy and challenging it was to identify and categorize each pixel compared with the training pixels from the same class. Consequently, an assumption on the density of seagrass patches in certain areas is possible provided a proper in-situ dataset for validation. Therefore, the core of this study is the definition of PUNC as it is the foundation for the computer science procedures and potentially, decision making by policy makers, as stated above.

4.3. Biases of the method and uncertainties of uncertainties

In order to be transparent and objective with the findings of this study, an acknowledgement of certain biases is required. Firstly, in the case of the Wakatobi classification, the validation dataset was derived from the same dataset as the training data. This decision was made due to the lack of field data from an independent source that would serve as validation dataset. Nonetheless and beside not achieving better accuracies, the classification models in Wakatobi are able to map and highlight areas with high or low uncertainty in regards to the classification outcome. Therefore, we aim to experiment more with PS data in the future, with independent training and validation datasets, and also run the workflow in temperate waters. The application in temperate waters is essential since the study sites are geospatially limited to the tropics where the ocean dynamics, water properties and behaviours are different.

Lastly, the size of the training points plays an important role as it must be big enough and represents equally all classes in order to be divided for the creation of the training subsets. As shown in the results, the average uncertainty of the best ensemble models per class is higher than the average uncertainty a standard classification. To further investigate this phenomenon, spatial analysis is needed to come to a better geo-spatial understanding of the new imported training data in each loop and their overall impact to the range of the training dataset values. An increase in the complexity of the model, as the presented alternative retraining workflow, will also increase the uncertainty (Abdar et al., 2021). Unfortunately though and despite the complexity of the task at hand, the small size of the training data per subset limits the flow of data that aim to help the classifier to adjust itself. Consequently, retraining the model by importing two to ten new points is not expected

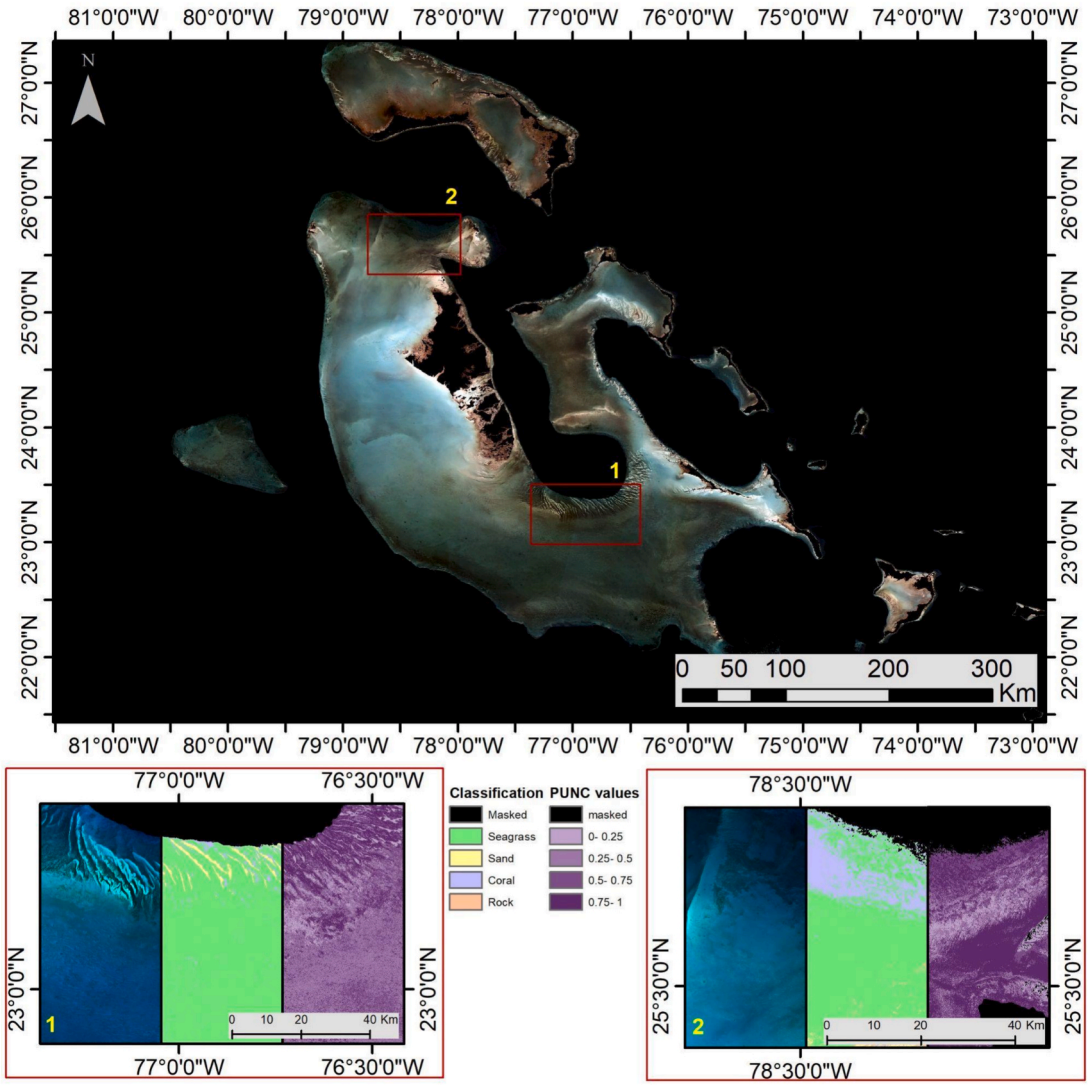

Fig. 2. Study case 1: Multi-temporal S2 composite of Bahamas national extent in true-color arrangement (RGB). The panels in the zoom-in windows and from left to right are the RGB, classifcation and, PUNC composites.

to significantly boost the accuracy scores.

4.4. Future prospects

This novel approach to the estimation of spatially-explicit uncertainty aims to produce and exploit spatial information on the noise that is introduced to the model. Towards that perspective, we are also working on the application of the presented method to temperate waters and to ML products with continuous distribution like Satellite Derived Bathymetries. As the estimation of the probabilities from such a distribution requires the implication of integrals with the same grade as the number of the spectral channels involved, a probability density function estimation is used in an attempt to reduce memory and computation costs.

Also of future interest is the identification of training points in time series in the context of exploring the temporal scalability of PUNC, and the density given the validation will occur with in-situ historical density data. Once achieved, change detection and monitoring of cover across time will be limited in a smaller scale by the absence or small number of field data. Eventually, we expect the creation of a function that will be able to sample training data from an image in context of their contribution to the ML process at hand based on their spectral and PUNC values, and the distribution of the sampled data. Hence, the small size issue of training data as described in 4.3 is expected to be addressed.

5. Conclusions

In conclusion, in this work we have established the efficacy of the presented workflow (chapter 2.3) in supporting monitoring and policy-making decisions, and ML procedures by minimizing the noise that is associated with training data. Overall, our method is not only able to produce a map that shows areas with potential misclassifications, but also provides information for a selection of training data that helps the model to adjust with the data at hand. Our findings indicate an improvement of the overall accuracy and a slight boost in the user's and producer's accuracy scores for the seagrass class in classification of The Bahamas. However, for Wakatobi the results are not reliable due to overstimation. Under these circumstances, we expect that spatially-explicit uncertainty may potentially prove a worthy tool for policy makers. As demonstrated, PUNC can spatially showcase the accuracy which is crucial for decision making of not only the creation of measurements for the protection and sustainability of meadows, but also for any related estimations based on a benthic habitat map.

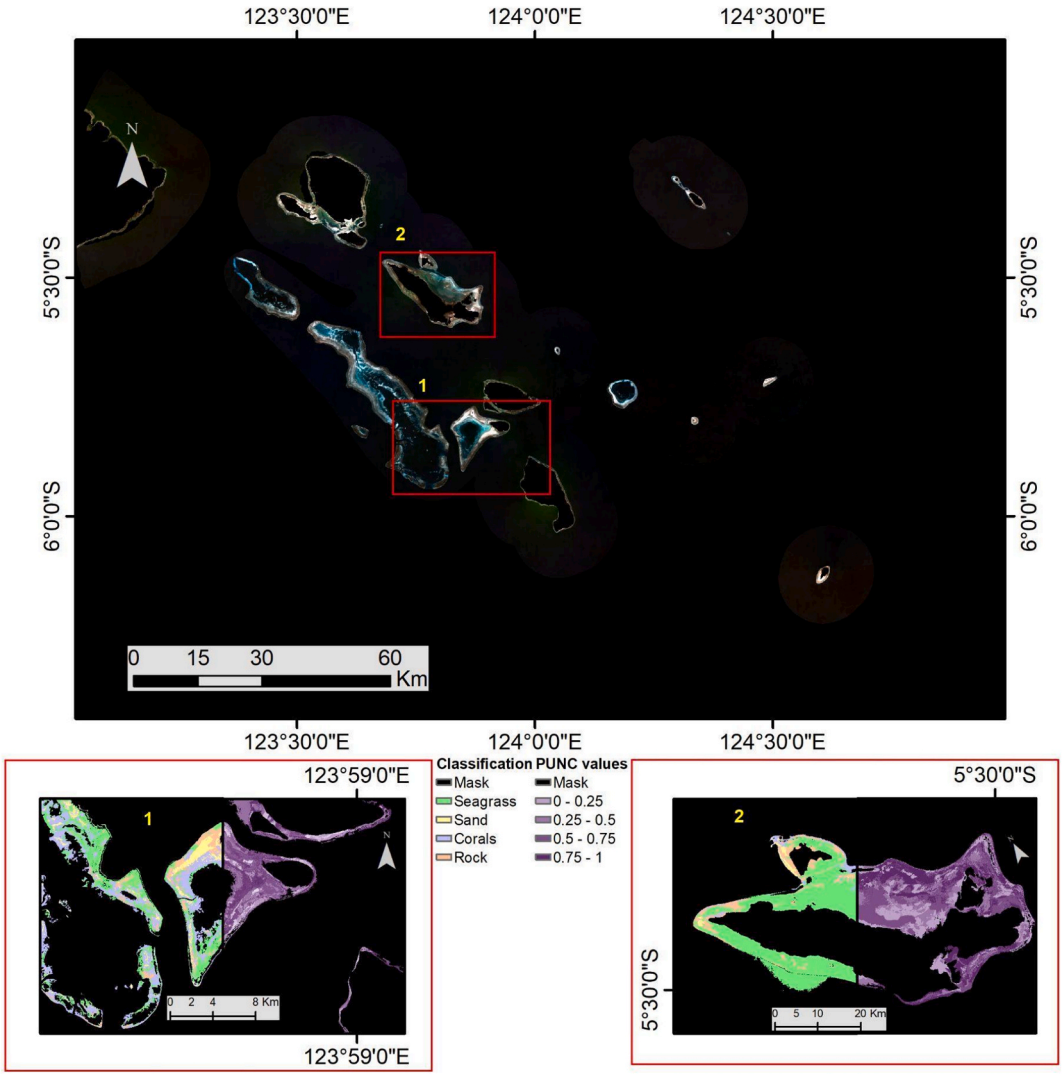

Fig. 3. Study case 2: Multi-temporal PS composite of Wakatobi archipelago coastal extent in true-color arrangement (RGB). The panels in the zoom-in windows and from left to right are the classification and PUNC composites.

CRediT authorship contribution statement

Spyridon Christofilakos: Writing – original draft, Visualization, Validation, Software, Methodology, Investigation, Formal analysis, Data curation, Conceptualization. **Alina Blume:** Writing – review & editing, Resources, Methodology, Formal analysis, Data curation. **Avi Putri Pertiwi:** Writing – review & editing, Resources, Methodology, Formal analysis, Data curation. **Chengfa Benjamin Lee:** Writing – review & editing, Resources, Methodology. **Dimosthenis Traganos:** Writing – review & editing, Supervision, Project administration, Funding acquisition. **Peter Reinartz:** Writing – review & editing, Supervision, Project administration, Funding acquisition.

Funding

S.C. is supported by the DLR-DAAD Research Fellowship (No. 57575487).

Declaration of competing interest

The authors declare that they have no known competing financial interests or personal relationships that could have appeared to influence the work reported in this paper.

Acknowledgments

We thank the EU for the Sentinel-2 program and Planet for their NICFI datasets as they both provide publicly available data for better monitoring and understanding of our planet. We also thank Allen Coral Atlas team for their free imagery, maps and monitoring of the world's tropical coral reefs. Finally, we would like to thank Miguel Pato for his help and support during the review process as well as the anonymous reviewers for their critical comments to improve the manuscript..

Appendix A. Supplementary material

Supplementary data to this article can be found online at https://doi.org/10.1016/j.jag.2025.104670.

Data availability

The data that has been used is confidential.

References

Abdar, M., Pourpanah, F., Hussain, S., Rezazadegan, D., Liu, L., Ghavamzadeh, M., Fieguth, P., Cao, X., Khosravi, A., Acharya, U.R., Makarenkov, V., Nahavandi, S., 2021. A review of uncertainty quantification in deep learning: Techniques,

applications and challenges. Inf. Fusion 76, 243–297. https://doi.org/10.1016/j.inffus.2021.05.008.
Alongi, D.M., Murdiyarso, D., Fourqurean, J.W., Kauffman, J.B., Hutahaean, A., Crooks, S., Lovelock, C.E., Howard, J., Herr, D., Fortes, M., Pidgeon, E., Wagey, T., 2016. Indonesia's blue carbon: a globally significant and vulnerable sink for seagrass and mangrove carbon. Wetl. Ecol. Manag. 24 (1), 3–13. https://doi.org/10.1007/s11273-015-9446-y.
Ayers, J.M., Strutton, P.G., Coles, V.J., Hood, R.R., Matear, R.J., 2014. Indonesian throughflow nutrient fluxes and their potential impact on Indian Ocean productivity. Geophys. Res. Lett. 41 (14), 5060–5067. https://doi.org/10.1002/2014GL060593.
Blaschke, T., Hay, G.J., Kelly, M., Lang, S., Hofmann, P., Addink, E., Feitosa, R.Q., van der Meer, F., van der Werff, H., van Coillie, F., Tiede, D., 2014. Geographic object-based image analysis: a new paradigm in remote sensing and geographic information science. ISPRS J. Photogramm. Remote Sens. 87 (1), 180–191. https://doi.org/10.1016/j.isprsjprs.2013.09.014.
Blume, A., Pertiwi, A.P., Lee, C.B., Traganos, D., 2023. Bahamian seagrass extent and blue carbon accounting using Earth observation. Front. Mar. Sci. 10, 1058460. https://doi.org/10.3389/fmars.2023.1058460.
Breiman, L., 2001. Random forests. Mach. Learn. 45 (1), 5–32. https://doi.org/10.1023/A:1010933404324.
Donchyts, G., Schellekens, J., Winsemius, H., Eisemann, E., van de Giesen, N., 2016. A 30 m resolution surface water mask including estimation of positional and thematic differences using landsat 8, SRTM and OpenStreetMap: a case study in the murray-darling Basin, Australia. Remote Sens. 8 (5), 386. https://doi.org/10.3390/RS8050386.
Doukari, M., Topouzelis, K., 2022. Overcoming the UAS limitations in the coastal environment for accurate habitat mapping. Remote Sens. Appl.: Soc. Environ. 26, 100726. https://doi.org/10.1016/J.RSASE.2022.100726.
Doxani, G., Vermote, E., Roger, J.C., Gascon, F., Adriaensen, S., Frantz, D., Hagolle, O., Hollstein, A., Kirches, G., Li, F., Louis, J., Mangin, A., Pahlevan, N., Pflug, B., Vanhellemont, Q., 2018. Atmospheric correction inter-comparison exercise. Remote Sens. 10 (2), 352. https://doi.org/10.3390/RS10020352.
Duarte, C.M., 2002. The future of seagrass meadows. Environ. Conserv. 29 (2), 192–206. https://doi.org/10.1017/S0376892902000127.
Duarte, C.M., Middelburg, J.J., Caraco, N., 2005. Major role of marine vegetation on the oceanic carbon cycle. Biogeosciences 2.
Duffy, J., 2006. Biodiversity and the functioning of seagrass ecosystems. Mar. Ecol. Prog. Ser. 311, 233–250. https://doi.org/10.3354/meps311233.
Economic Commission for Latin America and the Caribbean (2020). Ocean sustainability for prosperity and resilience issue 3. Retrieved September 27, 2023, from https://repositorio.cepal.org/server/api/core/bitstreams/c689042d-2290-4160-8c34-7bdcdc6a9ab0/content.
Edinger, E.N., Jompa, J., Limmon, G.V., Widjatmoko, W., Risk, M.J., 1998. Reef degradation and coral biodiversity in indonesia: Effects of land-based pollution, destructive fishing practices and changes over time. Marine Pollut. Bull. 36 (8), 617–630. https://doi.org/10.1016/S0025-326X(98)00047-2.
Ferrol-Schulte, D., Gorris, P., Baitoningsih, W., Adhuri, D.S., Ferse, S.C.A., 2015. Coastal livelihood vulnerability to marine resource degradation: a review of the Indonesian national coastal and marine policy framework. Marine Policy 52, 163–171. https://doi.org/10.1016/J.MARPOL.2014.09.026.
Gallagher, A.J., Brownscombe, J.W., Alsudairy, N.A., Casagrande, A.B., Fu, C., Harding, L., Harris, S.D., Hammerschlag, N., Howe, W., Huertas, A.D., Kattan, S., Kough, A.S., Musgrove, A., Payne, N.L., Phillips, A., Shea, B.D., Shipley, O.N., Sumaila, U.R., Hossain, M.S., Duarte, C.M., 2022. Tiger sharks support the characterization of the world's largest seagrass ecosystem. Nat. Commun. 13 (1), 1–10. https://doi.org/10.1038/s41467-022-33926-1.
Gascon, F., Bouzinac, C., Thépaut, O., Jung, M., Francesconi, B., Louis, J., Lonjou, V., Lafrance, B., Massera, S., Gaudel-Vacaresse, A., Languille, F., Alhammoud, B., Viallefont, F., Pflug, B., Bieniarz, J., Clerc, S., Pessiot, L., Trémas, T., Cadau, E., Fernandez, V., 2017. Copernicus sentinel-2A calibration and products validation status. Remote Sens. 9 (6), 584. https://doi.org/10.3390/RS9060584.
Guerrero-Font, E., Bonin-Font, F., Martin-Abadal, M., Gonzalez-Cid, Y., Oliver-Codina, G., 2021. Sparse Gaussian process for online seagrass semantic mapping. Expert Syst. Appl. 170, 114478. https://doi.org/10.1016/J.ESWA.2020.114478.
Hartoni, H., Siregar, V.P., Wouthuyzen, S., Agus, S.B., 2021. Object based classification of benthic habitat using Sentinel 2 imagery by applying with support vector machine and Random forest algorithms in shallow waters of Kepulauan Seribu, Indonesia. Biodiversitas J. Biol. Diversity 23, 514–520. https://doi.org/10.13057/biodiv/d230155.
Hossain, M.S., Hashim, M., 2019. Potential of Earth Observation (EO) technologies for seagrass ecosystem service assessments. Int. J. Appl. Earth Observ. Geoinform. 77, 15–29. https://doi.org/10.1016/j.jag.2018.12.009.
Infantes, E., Hoeks, S., Adams, M.P., van der Heide, T., van Katwijk, M.M., Bouma, T.J., 2022. Seagrass roots strongly reduce cliff erosion rates in sandy sediments. Marine Ecology Progress Series 700, 1–12. https://doi.org/10.3354/meps14196.
Kovacs, E., Roelfsema, C., Lyons, M., Zhao, S., Phinn, S., 2018. Seagrass habitat mapping: how do Landsat 8 OLI, Sentinel-2, ZY-3A, and Worldview-3 perform? Remote Sens. Lett. 9 (7), 686–695. https://doi.org/10.1080/2150704X.2018.1468101.
Kuhwald, K., Schneider von Deimling, J., Schubert, P., Oppelt, N., 2022. How can Sentinel-2 contribute to seagrass mapping in shallow, turbid Baltic Sea waters? Remote Sens. Ecol. Conserv. 8 (3), 328–346. https://doi.org/10.1002/RSE2.246.
Lang, N., Kalischek, N., Armston, J., Schindler, K., Dubayah, R., Wegner, J.D., 2022. Global canopy height regression and uncertainty estimation from GEDI LIDAR waveforms with deep ensembles. Remote Sens. Environ. 268, 112760. https://doi.org/10.1016/j.rse.2021.112760.
Lavery, P.S., Mateo, M.Á., Serrano, O., Rozaimi, M., 2013. Variability in the carbon storage of seagrass habitats and its implications for global estimates of blue carbon ecosystem service. PLOS ONE 8 (9), e73748. https://doi.org/10.1371/JOURNAL.PONE.0073748.
Lee, C.B., Martin, L., Traganos, D., Antat, S., Baez, S.K., Cupidon, A., Faure, A., Harlay, J., Morgan, M., Mortimer, J.A., Reinartz, P., Rowlands, G., 2023. Mapping the national seagrass extent in seychelles using planetscope NICFI data. Remote Sens. 15 (18), 4500. https://doi.org/10.3390/RS15184500.
Lee, C.B., Traganos, D., Reinartz, P., 2022. A simple cloud-native spectral transformation method to disentangle optically shallow and deep waters in sentinel-2 images. Remote Sens. 14 (3), 590. https://doi.org/10.3390/RS14030590.
Li, Q., Jin, R., Ye, Z., Gu, J., Dan, L., He, J., Christakos, G., Agusti, S., Duarte, C.M., Wu, J., 2022. Mapping seagrass meadows in coastal China using GEE. Geocarto Int. 37 (26), 12602–12617. https://doi.org/10.1080/10106049.2022.2070672.
Litsi-Mizan, V., Efthymiadis, P.T., Gerakaris, V., Serrano, O., Tsapakis, M., Apostolaki, E. T., 2023. Decline of seagrass (Posidonia oceanica) production over two decades in the face of warming of the Eastern Mediterranean Sea. New Phytologist 239 (6), 2126–2137. https://doi.org/10.1111/nph.19084.
Louis, J., Pflug, B., Main-Knorn, M., Debaecker, V., Mueller-Wilm, U., Iannone, R.Q., Giuseppe Cadau, E., Boccia, V., Gascon, F., 2019. Sentinel-2 Global Surface Reflectance Level-2a Product Generated with Sen2Cor. In: IGARSS 2019–2019 IEEE International Geoscience and Remote Sensing Symposium, pp. 8522–8525. https://doi.org/10.1109/IGARSS.2019.8898540.
Lyons, M., Larsen, K., & Skone, M. (2022). *CoralMapping/AllenCoralAtlas: DOI for paper at ~ v1.3.* . Zenodo. DOI: 10.5281/ZENODO.6622015.
Orth, R.J., Heck, K.L., 2023. The dynamics of seagrass ecosystems: history, past accomplishments, and future prospects. Estuaries and Coasts. https://doi.org/10.1109/TSMC.1979.4310076.
Otsu, N., 1979. A Threshold selection method from gray-level histograms. IEEE Trans. Syst., Man, Cybernetics 9 (1), 62–66. https://doi.org/10.1109/TSMC.1979.4310076.
Pahlevan, N., Mangin, A., Balasubramanian, S.V., Smith, B., Alikas, K., Arai, K., Barbosa, C., Bélanger, S., Binding, C., Bresciani, M., Giardino, C., Gurlin, D., Fan, Y., Harmel, T., Hunter, P., Ishikaza, J., Kratzer, S., Lehmann, M.K., Ligi, M., Warren, M., 2021. ACIX-Aqua: a global assessment of atmospheric correction methods for Landsat-8 and Sentinel-2 over lakes, rivers, and coastal waters. Remote Sens. Environ. 258, 112366. https://doi.org/10.1016/J.RSE.2021.112366.
Pal, M., 2005. Random forest classifier for remote sensing classification. Int. J. Remote Sens. 26 (1), 217–222. https://doi.org/10.1080/01431160412331269698.
Panjaitan, J. P., & Hamidah, M. (2023) IOP Conf. Ser.: Earth Environ. Sci. 1251 012065 DOI: 10.1088/1755-1315/1251/1/012065.
Papenbrock, J., Teichberg, M., 2023. Editorial: current advances in seagrass research. Front. Plant Sci. 14, 1196437. https://doi.org/10.3389/fpls.2023.1196437.
Paul, M., 2018. The protection of sandy shores – can we afford to ignore the contribution of seagrass? Marine Pollut. Bull. 134, 152–159. https://doi.org/10.1016/J.MARPOLBUL.2017.08.012.
Perez, D., Islam, K., Hill, V., Zimmerman, R., Schaeffer, B., Shen, Y., Li, J., 2020. Quantifying seagrass distribution in coastal water with deep learning models. Remote Sens. 12 (10), 1581. https://doi.org/10.3390/RS12101581.
Pertiwi, A.P., Lee, C.B., Traganos, D., 2021. Cloud-native coastal turbid zone detection using multi-temporal sentinel-2 data on google earth engine. Front. Marine Sci. 8, 699055. https://doi.org/10.3389/FMARS.2021.699055.
Planet Labs PBC (2018). Planet Application Program Interface: In space for Life on Earth. https://api.planet.com.
Potouroglou, M., Bull, J.C., Krauss, K.W., Kennedy, H.A., Fusi, M., Daffonchio, D., Mangora, M.M., Githaiga, M.N., Diele, K., Huxham, M., 2017. Measuring the role of seagrasses in regulating sediment surface elevation. Scient. Rep. 7 (1). https://doi.org/10.1038/s41598-017-12354-y.
Poursanidis, D., Topouzelis, K., Chrysoulakis, N., 2018. Mapping coastal marine habitats and delineating the deep limits of the Neptune's seagrass meadows using very high resolution Earth observation data. Int. J. Remote Sens. 39 (23), 8670–8687. https://doi.org/10.1080/01431161.2018.1490974.
Poursanidis, D., Traganos, D., Reinartz, P., Chrysoulakis, N., 2019. On the use of Sentinel-2 for coastal habitat mapping and satellite-derived bathymetry estimation using downscaled coastal aerosol band. Int. J. Appl. Earth Observ. Geoinform. 80, 58–70. https://doi.org/10.1016/J.JAG.2019.03.012.
Roelfsema, C.M., Lyons, M., Murray, N., Kovacs, E.M., Kennedy, E., Markey, K., Borrego-Acevedo, R., Ordoñez, A., Say, C., Tudman, P., Roe, M., Wolff, J., Traganos, D., Asner, G.P., Bambic, B., Free, B., Fox, H.E., Lieb, Z., Phinn, S.R., 2021. Workflow for the generation of expert-derived training and validation data: a view to global scale habitat mapping. Front. Marine Sci. 8, 643381. https://doi.org/10.3389/fmars.2021.643381.
Sayer, A.M., Govaerts, Y., Kolmonen, P., Lipponen, A., Luffarelli, M., Mielonen, T., Patadia, F., Popp, T., Povey, A.C., Stebel, K., Witek, M.L., 2020. A review and framework for the evaluation of pixel-level uncertainty estimates in satellite aerosol remote sensing. Atmosph. Measure. Techn. 13, 373–404. https://doi.org/10.5194/amt-13-373-2020.
Shannon, C.E., 1948. A mathematical theory of communication. Bell Syst. Tech. J. 27 (3), 379–423. https://doi.org/10.1002/J.1538-7305.1948.TB01338.X.
Slattery, M., Lesser, M.P., 2019. The bahamas and cayman islands. Coral Reefs of the World 12, 47–56. https://doi.org/10.1007/978-3-319-92735-0_3.
Sprintall, J., Gordon, A.L., Koch-Larrouy, A., Lee, T., Potemra, J.T., Pujiana, K., Wijffels, S.E., 2014. The Indonesian seas and their role in the coupled ocean–climate system. Nat. Geosci. 7 (7), 487–492. https://doi.org/10.1038/ngeo2188.

Taufiqurrahman, E., Wahyudi, A.J., Masumoto, Y., 2020. The Indonesian throughflow and its impact on biogeochemistry in the Indonesian seas. ASEAN J. Sci. Technol. Develop. 37 (1), 29–35. https://doi.org/10.29037/ajstd.596.

Topouzelis, K., Makri, D., Stoupas, N., Papakonstantinou, A., Katsanevakis, S., 2018. Seagrass mapping in Greek territorial waters using Landsat-8 satellite images. Int. J. Appl. Earth Observ. Geoinform. 67, 98–113. https://doi.org/10.1016/J.JAG.2017.12.013.

Traganos, D., Aggarwal, B., Poursanidis, D., Topouzelis, K., Chrysoulakis, N., Reinartz, P., 2018. Towards global-scale seagrass mapping and monitoring using sentinel-2 on google earth engine: the case study of the aegean and Ionian seas. Remote Sens. 10 (8), 1227. https://doi.org/10.3390/RS10081227.

Traganos, D., Lee, C.B., Blume, A., Poursanidis, D., Čižmek, H., Deter, J., Mačić, V., Montefalcone, M., Pergent, G., Pergent-Martini, C., Ricart, A.M., Reinartz, P., 2022a. Spatially explicit seagrass extent mapping across the entire mediterranean. Front. Marine Sci. 9. https://doi.org/10.3389/fmars.2022.871799.

Traganos, D., Pertiwi, A.P., Lee, C.B., Blume, A., Poursanidis, D., Shapiro, A., 2022b. Earth observation for ecosystem accounting: spatially explicit national seagrass extent and carbon stock in Kenya, Tanzania, Mozambique and Madagascar. Remote Sens. Ecol. Conserv. 8 (6), 778–792. https://doi.org/10.1002/RSE2.287.

Tran, B.N., van der Kwast, J., Seyoum, S., Uijlenhoet, R., Jewitt, G., Mul, M., 2023. Uncertainty assessment of satellite remote-sensing-based evapotranspiration estimates: a systematic review of methods and gaps. Hydrol. Earth Syst. Sci. 27, 4505–4528. https://doi.org/10.5194/hess-27-4505-2023.

United Nations (2015). *Transforming our World: The 2030 agenda for sustainable development.* https://sustainabledevelopment.un.org/post2015/transformingourworld/publication.

Unsworth, R. K. F., Clifton, J., & Smith, D. (2010). Seagrass meadows of the Wakatobi National Park. In J. Clifton, R. K. F. Unsworth, & D. J. Smith (Eds.), *Seagrass meadows of the Wakatobi National Park* [PDF]. https://www.academia.edu/2673922/Seagrass_meadows_of_the_Wakatobi_National_Park.

Unsworth, R.K.F., Nordlund, L.M., Cullen-Unsworth, L.C., 2019. Seagrass meadows support global fisheries production. Conserv. Lett. 12 (1). https://doi.org/10.1111/conl.12566.

Velegrakis, A.F., Chatzistratis, D., Chalazas, T., Armaroli, C., Schiavon, E., Alves, B., Grigoriadis, D., Hasiotis, T., Ieronymidi, E., 2024. Earth observation technologies, policies and legislation for the coastal flood risk assessment and management: a European perspective. Anthropocene Coasts 7, 3. https://doi.org/10.1007/s44218-024-00037-x.

Wicaksono, P., Lazuardi, W., 2018. Assessment of PlanetScope images for benthic habitat and seagrass species mapping in a complex optically shallow water environment. Int. J. Remote Sens. 39 (17), 5739–5765. https://doi.org/10.1080/01431161.2018.1506951.

Zhang, S., Hu, C., Barnes, B.B., Harrison, T.N., 2022. Monitoring *Sargassum* inundation on beaches and nearshore waters using planetscope/dove observations. IEEE Geosci. Remote Sens. Lett. 19, 1–5. https://doi.org/10.1109/LGRS.2022.3148684.